We are IntechOpen, the world's leading publisher of Open Access books Built by scientists, for scientists

4,800
Open access books available

122,000
International authors and editors

135M
Downloads

Our authors are among the

154
Countries delivered to

TOP 1%
most cited scientists

12.2%
Contributors from top 500 universities

WEB OF SCIENCE™

Selection of our books indexed in the Book Citation Index in Web of Science™ Core Collection (BKCI)

Interested in publishing with us?
Contact book.department@intechopen.com

Numbers displayed above are based on latest data collected.
For more information visit www.intechopen.com

Chapter 15

Wind Diesel Hybrid Power System with Hydrogen Storage

Mamadou Lamine Doumbia, Karim Belmokhtar and Kodjo Agbossou

Additional information is available at the end of the chapter

http://dx.doi.org/10.5772/52341

1. Introduction

By 2050 the demand for energy could double or even triple as the global population grows and developing countries expand their economies. Energy prices, supply uncertainties, and environmental concerns are driving many countries to rethink their energy mix. The International Energy Agency's Energy Technology Perspectives2008publication projects that energy sector emissions of greenhouse gases (GHGs) will increase by 130% over 2005 levels, by 2050, in the absence of new policies (IEA, 2008).

Renewable energy is part of the solution for the energy problem, and wind energy is one of the cost-effective options for the generation of electricity. The main applications are the generation of electricity and water pumping.

By the end of 2007, in the world, there were around 100,000 wind turbines installed in wind farms, with an installed capacity of 94,000 megawatts, which generated around 300 TWh/year. Wind energy is now part of national policies for generation of electricity in many countries (Vaughn Nelson, 2009).

In 2007, in Europe there were 57,000 MW installed wind power, which generated 3.7% of the electrical demand. The European goal is 20% of electricity generated by renewables by 2020, of which 12–14% would be from wind. In 2010, wind energy provided for nearly 26% of electricity consumption in Denmark, more than 15% in Portugal and Spain, 14% in Ireland and nearly 9% in Germany, over 4% of all European Union (EU) electricity, and nearly 2.9% in the United States (US Department of Energy, 2011). In the future, many countries around the world are likely to experience similar penetration levels as wind power is increasingly considered not only a means to reduce CO_2 emissions but also an interesting economic alter-

native in areas with appropriate wind speeds. Since 2000, cumulative installed capacity has grown at an average rate of around 30% per year. In 2008, more than 27 GW of capacity were installed in more than 50 countries, bringing global capacity onshore and offshore to 121 GW. Wind energy in 2008 was estimated by the Global Wind Energy Council to have generated some 260 million megawatt hours of electricity. Applications for generation of electricity are divided into the following categories: utility-scale wind farms and small wind turbines (less than 100 kW).

Currently, for remote communities and rural industry the standard is diesel generators. Remote electric power is estimated at over 11 GW, with 150,000 diesel gensets, ranging in size from 5 to 1,000 kW. In Canada, there are more than 800 diesel gensets, with a combined installed rating of over 500 MW in more than 300 remote communities (Vaughn Nelson, 2009). Diesel generators are inexpensive to install; however, they are expensive to operate and maintain, and major maintenance is needed from every 2,000 to 20,000 hours, depending on the size of the diesel genset.

Wind–diesel is considered because of the high costs for generating power in isolated systems. In near future, the market of wind–diesel systems will grow up because of the high cost of diesel fuel. Wind–diesel power systems can vary from simple designs in which wind turbines are connected directly to the diesel grid, with a minimum of additional features, to more complex systems.

There are a number of problems in integrating a wind turbine to an existing diesel genset: voltage and frequency control, frequent stop–starts of the diesel, utilization of surplus energy, and the use and operation of a new technology. These problems vary by the amount of penetration. Wind turbines at low penetration can be added to existing diesel power without many problems, as it is primarily a fuel saver. However, for high wind penetration, storage is needed. Moreover, one of the major drawbacks of wind energy is its unpredictability and intermittency. So, to supply better consumers' energy needs, wind systems have to operate with storage devices. Several energy storage methods have been in development over the past several years. This includes compressed air, pumped hydro, flow battery flywheel, hydrogen storage, etc. It has been proved (E.I. Zoulias, N. Lymberopoulos, 2008; Nelson et al., 2006) that hydrogen can be effectively used as storage medium for intermittent renewable energy sources (RES)-based autonomous power systems. More specifically, excess of RES energy produced from such systems at periods of low demand can be stored in the form of hydrogen, which will be used upon demand during periods when the wind energy is not available.

For many years, Hydrogen Research Institute (HRI) has developed a renewable photovoltaic/wind energy system based on hydrogen storage(M. L. Doumbiaet al., 2009; K. Agbossou et al., 2004). The system consists of a 10 kW wind turbine generator (WTG) and a 1 kW solar photovoltaic (PV) array as primary energy sources, a battery bank, an 5 kW electrolyzer, a 5 kW fuel cell stack, different power electronics interfaces for control and voltage adaptation purposes, a measurement and monitoring system. This renewable energy system is scaled for residential applications size and can be operated in stand-alone or grid-connected mode and different control strategies can be developed.

http://dx.doi.org/10.5772/52341

Numerical modelling is an important part of the design, assessment, implementation and evaluation of autonomous power systems with wind power.

This chapter is devoted to a large scale wind-diesel Hybrid Power System (HPS) applications. It presents theoretical analysis, modelling and control of Wind Energy Conversion Systems (WECS) connected to an autonomous power system with hydrogen storage. The wind generator under study is a Doubly Fed Induction Generator (DFIG) type. The models of the main components (mainly wind turbine, generator, diesel genset, electrolyzer) will be derived. The wind turbine's maximum power point tracking technique will be presented and a power transfer strategy in the interconnected system will be analysed. Performance of the control method is validated to maintain the hybrid power system's frequency. The effectiveness of the proposed hybrid system is validated by simulation using Matlab/ Simulink/ SimPowerSystems environment. The Hybrid Power System (HPS) is composed of a 600 kW diesel genset, three 190 kW wind turbines, three 80 kW alkaline electrolyzers and a 610 kW maximum load.

2. Wind-diesel power system with hydrogen storage

The structures of Hybrid Power System (HPS) can be classified into two categories: AC coupled and DC-coupled (T. Zhou, 2009).

In an AC-coupled HPS, all sources are connected to a main AC-bus before being connected to the grid. In AC-coupled structure, different sources can be located anywhere in the microgrid with a long distance from each other. However, the voltage and the frequency of the main AC bus should be well controlled in order to ensure the stability of the system and the compatibility with the utility network.

In a DC-coupled HPS, all sources are connected to a main DC-bus before being connected to the grid through a main inverter. In a DC-coupled structure, the voltage and the frequency of the grid are independent from those of each source.

However, not all HPSs can be classified into AC or DC-coupled system, since it is possible to have both coupling methods, then a Mixed HPS is obtained. In this case, some advantages can be taken from both structures.

The wind-diesel HPS configuration studied in this work is represented in Fig. 1.

2.1. Wind turbine

Wind turbines come in different sizes and types, depending on power generating capacity and the rotor design deployed. Small wind turbines with output capacities below 10 kW are used primarily for residences, telecommunications dishes, and irrigation water pumping applications. Utility-scale wind turbines have high power ratings ranging from 100 kW to 5 MW. Current wind farms with large capacity wind turbine installations are

capable of generating electricity in excess of 500M MW for utility companies (Vaughn Nelson, 2009).

Modern wind turbines are classified into two configurations: horizontal-axis wind turbines (HAWTs) and vertical-axis wind turbines (VAWTs), depending on rotor operating principles. The VAWT configuration employs the Darrieus model named for the famous French inventor.

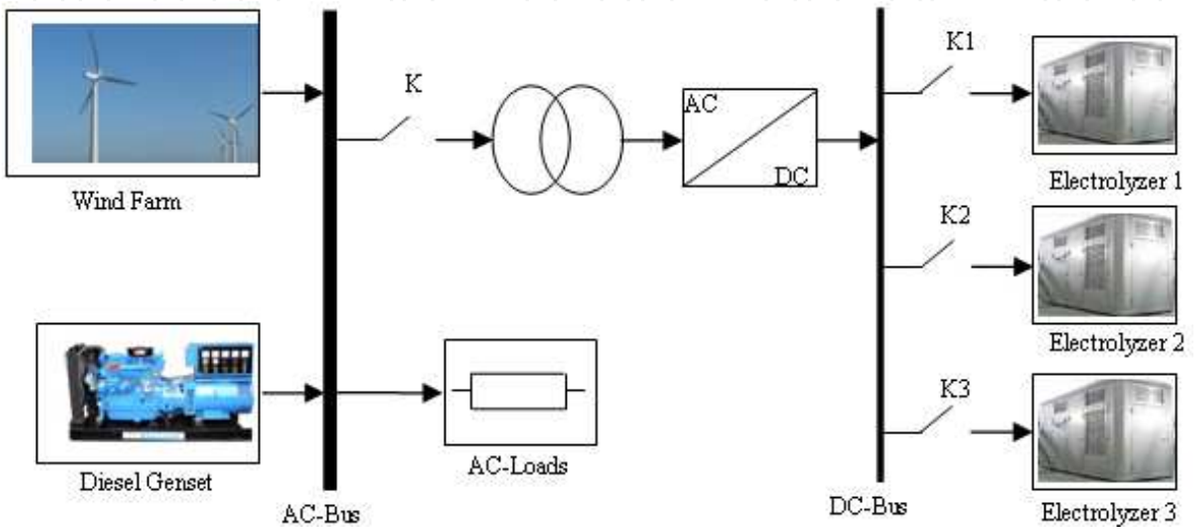

Figure 1. Wind-diesel Hybrid Power System with hydrogen production

HAWTs with two or three blades are the most common. Wind blowing over the propeller blades causes the blades to "lift" and rotate at low speeds. Wind turbines using three blades are operated "upwind" with rotor blades facing into the wind. The tapering of rotor blades is selected to maximize the kinetic energy from the wind. Optimum wind turbine performance is strictly dependent on blade taper angle and the installation height of the turbine on the tower (Vaughn Nelson, 2009).

According to Albert Betz, the mechanical power P_m captured by the turbine from the wind for a given wind speed v_w is computed by the following expression (I. Munteanu et al., 2008; N.M. Miller et al., 2008).

$$P_m = \frac{1}{2}\rho A C_p(\lambda,\beta) v_w^3 \tag{1}$$

$\rho$is the air density in kg/m^3; $A=\pi R^2$is the area in m^2 swept by the blade; $R$is the radius of the blade in m.

The aerodynamic model of a wind turbine can be determined by the $C_p(\lambda,\beta)$ curves. C_p is the power coefficient, which is function of both tip speed ratio λ and the blade pitch angle β. The tip speed ratio is given by:

http://dx.doi.org/10.5772/52341

$$\lambda = \frac{\Omega_r R}{v_w} \tag{2}$$

Ω_r represents the rotational speed of the wind turbine in *rad/sec*.

The maximum power coefficient C_p is determined by Betz as follows (S. Heier, 1998):

$$C_p^{\max}(\lambda, \beta) = \frac{16}{27} \approx 0.593 \tag{3}$$

Hence, even if power extraction without any losses were possible, only 59% of the wind power could be utilized by a wind turbine.

The power coefficient versus the ratio speed as shown in Fig. 2.

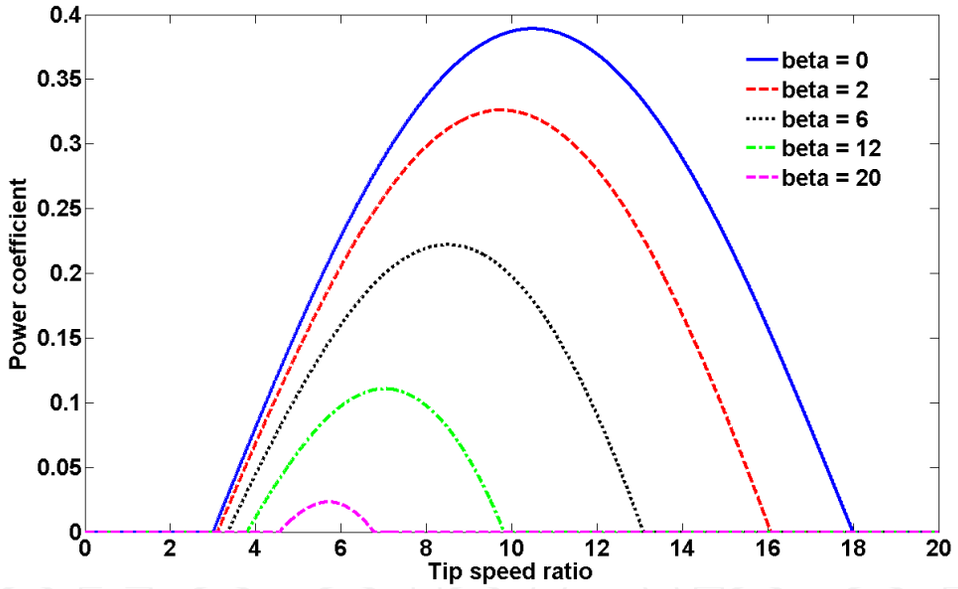

Figure 2. Coefficient of power versus ratio of speed

In our study, the mathematical representation of the power coefficient used for a wind turbine is given by:

$$C_p = 0.398.\sin\left(\frac{\pi(\lambda - 3)}{15 - 0.3\beta}\right) - 0.00394(\lambda - 2)\beta \tag{4}$$

In the aim to extract the maximum active power, the speed of the wind turbine must be adjusted to achieve the optimal value of the tip speed ratio. The block diagram of Fig. 3 shows the Maximum Power Point Tracking (MPPT) technique applied to the generator to produce maximum

power. If the wind speed is below the rated value, the WTG operates in the variable speed mode, and C_p is keep at its maximum value. In this operating mode, the pitch control is deactivated. When the wind speed is above the rated value, the pitch control is activated, in the aim to reduce the generated mechanical power (W. Qiao, W. Zhou et al., 2008).

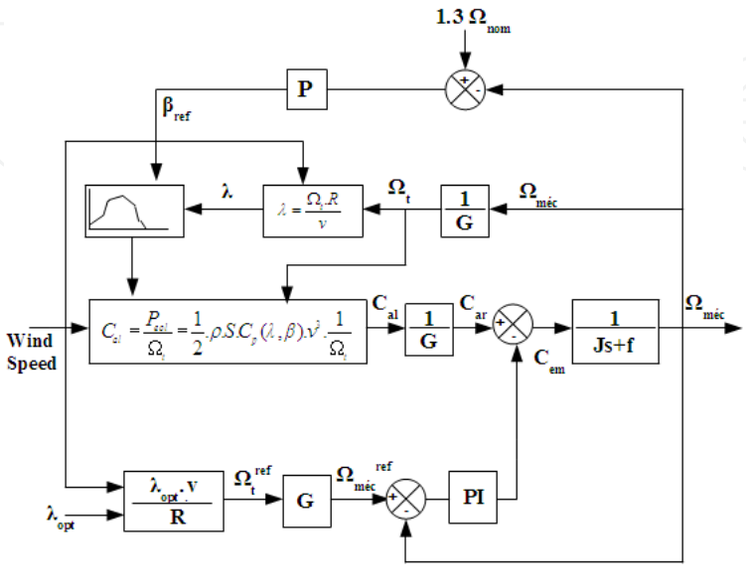

Figure 3. Block diagram of the control of the velocity of the DFIG with MPPT

2.2. Doubly-fed induction generator and its control

a. Doubly-Fed induction Generator

Today, the wind turbines on the market mix and match a variety of innovative concepts with proven technologies both for generators and for power electronics. Wind turbines can operate either with a fixed speed or a variable speed. Most commonly used types of wind turbines generators are asynchronous (induction) and synchronous generators. Among these technologies, asynchronous Doubly Fed Induction Generator (DFIG) has received much attention as one of preferred technology for wind power generation (Fig.4). The DFIG consists of a Wound Rotor Induction Generator (WRIG) with the stator windings directly connected to the constant-frequency three-phase grid and with the rotor windings mounted to a bidirectional back-to-back IGBT voltage source converter.The converter compensates the difference between the mechanical and electrical frequency by injecting a rotor current with a variable frequency.The power converter consists of two converters, the rotor-side converter and grid-side converter, which are controlled independently of each other.The main idea is that the rotor-side converter controls the active and reactive power by controlling the rotor current components, while the line-side converter controls the DC-link voltage and ensures a converter operation at unity power factor (i.e. zero reactive power). Compared to a full rated converter system, the use of DFIG in a wind turbine offers many advantages, such as reduction of inverter cost, the potential to control torque and a slight increase in efficiency of wind energy extraction. Depending on the operating

http://dx.doi.org/10.5772/52341

condition of the drive, power is fed into or out of the rotor: in an oversynchronous mode, it flows from the rotor via the converter to the grid, whereas it flows in the opposite direction in a subsynchronous mode. In both cases – subsynchronous and oversynchronous – the stator feeds energy into the grid (T. Ackermann, 2005).

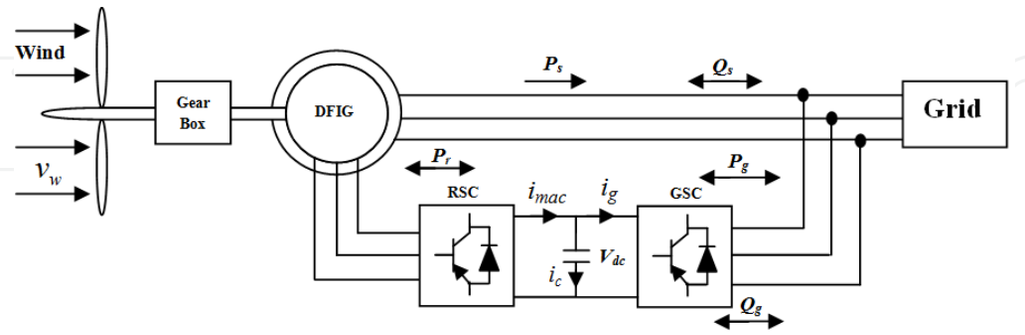

Figure 4. Structure of the DFIG based wind system

The stator and rotor voltages of the DFIG are given by the following expression (Y. Ren, H. Li and J. Zhou, 2009; R. G. De Almeida et al., 2004).

$$\begin{cases} v_{ds} = r_s i_{ds} + \dfrac{d\lambda_{ds}}{dt} - \omega_s \lambda_{qs} \\ v_{qs} = r_s i_{qs} + \dfrac{d\lambda_{qs}}{dt} + \omega_s \lambda_{ds} \\ v_{dr} = r_r i_{dr} + \dfrac{d\lambda_{dr}}{dt} - \omega_r \lambda_{qr} \\ v_{qr} = r_r i_{qr} + \dfrac{d\lambda_{qr}}{dt} + \omega_r \lambda_{dr} \end{cases} \tag{5}$$

r_s and r_r are respectively the resistance of the stator and rotor windings, and ω_s is the rotational speed of the synchronous reference frame.

$$\begin{cases} \lambda_{ds} = L_s i_{ds} + L_m i_{dr} \\ \lambda_{qs} = L_s i_{qs} + L_m i_{qr} \\ \lambda_{dr} = L_r i_{dr} + L_m i_{ds} \\ \lambda_{qr} = L_r i_{qr} + L_m i_{qs} \end{cases} \tag{6}$$

L_s and L_r represent respectively the self-inductance of the stator and the rotor windings, and L_m is the mutual inductance between the stator and the rotor windings.

The electromagnetic torque of the DFIG can be expressed as follow:

$$T_{em} = P(\lambda_{ds} i_{qs} - \lambda_{qs} i_{ds}) \tag{7}$$

P is the number of pole pairs.

To achieve independent control of the stator active power and stator reactive power, a vector-control approach is used. *d-q* axis connected to the stator's rotating field is chosen and quadratic component of the stator flux is set to zero. The power control is performed through the back to back converter connected to the rotor. Then, the stator voltages can be given according the rotor currents as (D. Aouzellag et al. 2006).

The stator's flux and current equations are:

$$\begin{cases} \lambda_{ds} = L_s i_{ds} + L_m i_{dr} = \Phi_s \\ \lambda_{qs} = L_s i_{qs} + L_m i_{qr} = 0 \end{cases} \tag{8}$$

$$\begin{cases} i_{ds} = \dfrac{\Phi_s}{L_s} - \dfrac{L_m}{L_s} i_{dr} \\ i_{qs} = -\dfrac{L_m}{L_s} i_{qr} \end{cases} \tag{9}$$

Fom equations (5) et (6), rotor's voltages can be rewritten as:

$$\begin{cases} v_{dr} = r_r i_{dr} + \dfrac{d\left(L_r i_{dr} + L_m i_{ds}\right)}{dt} - \omega_r \left(L_r i_{qr} + L_m i_{qs}\right) \\ v_{qr} = r_r i_{qr} + \dfrac{d\left(L_r i_{qr} + L_m i_{qs}\right)}{dt} + \omega_r \left(L_r i_{dr} + L_m i_{ds}\right) \end{cases} \tag{10}$$

$$\begin{cases} v_{dr} = r_r i_{dr} + L_r \dfrac{di_{dr}}{dt} + L_m \dfrac{di_{ds}}{dt} - \omega_r L_r i_{qr} + \omega_r L_m i_{qs} \\ v_{qr} = r_r i_{qr} + L_r \dfrac{di_{qr}}{dt} + L_m \dfrac{di_{qs}}{dt} + \omega_r L_r i_{dr} + \omega_r L_m i_{ds} \end{cases} \tag{11}$$

$$\begin{cases} v_{dr} = r_r i_{dr} + L_r \dfrac{di_{dr}}{dt} - L_m \dfrac{L_m di_{dr}}{L_s dt} - \omega_r L_r i_{qr} - \omega_r L_m \dfrac{L_m}{L_s} i_{qr} \\ v_{qr} = r_r i_{qr} + L_r \dfrac{di_{qr}}{dt} - L_m \dfrac{L_m di_{qr}}{L_s dt} + \omega_r L_r i_{dr} + \omega_r L_m \dfrac{\Phi_s}{L_s} - \omega_r L_m \dfrac{L_m}{L_s} i_{dr} \end{cases} \tag{12}$$

http://dx.doi.org/10.5772/52341

$$\begin{cases} v_{dr} = r_r i_{dr} + \left(L_r - \dfrac{L_m^{\,2}}{L_s} \right) \dfrac{di_{dr}}{dt} - \omega_r L_r i_{qr} - \omega_r \dfrac{L_m^{\,2}}{L_s} i_{qr} \\ v_{qr} = r_r i_{qr} + \left(L_r - \dfrac{L_m^{\,2}}{L_s} \right) \dfrac{di_{qr}}{dt} + \omega_r L_r i_{dr} + \omega_r L_m \dfrac{\Phi_s}{L_s} - \omega_r \dfrac{L_m^{\,2}}{L_s} i_{dr} \end{cases} \tag{13}$$

$$\begin{cases} v_{dr} = r_r i_{dr} + \left(L_r - \dfrac{L_m^{\,2}}{L_s} \right) \dfrac{di_{dr}}{dt} - \omega_r \left(L_r - \dfrac{L_m^{\,2}}{L_s} \right) i_{qr} \\ v_{qr} = r_r i_{qr} + \left(L_r - \dfrac{L_m^{\,2}}{L_s} \right) \dfrac{di_{qr}}{dt} + \omega_r \left(L_r - \dfrac{L_m^{\,2}}{L_s} \right) i_{dr} + \omega_r L_m \dfrac{\Phi_s}{L_s} \end{cases} \tag{14}$$

ω_r and ω_s are respectively rotor and stator parameters frequencies; s is the machine's slip.

As

$$\omega_r = s\omega_s$$

$$\begin{cases} v_{dr} = r_r i_{dr} + \left(L_r - \dfrac{L_m^{\,2}}{L_s} \right) \dfrac{di_{dr}}{dt} - s\omega_s \left(L_r - \dfrac{L_m^{\,2}}{L_s} \right) i_{qr} \\ v_{qr} = r_r i_{qr} + \left(L_r - \dfrac{L_m^{\,2}}{L_s} \right) \dfrac{di_{qr}}{dt} + s\omega_s \left(L_r - \dfrac{L_m^{\,2}}{L_s} \right) i_{dr} + g\omega_s L_m \dfrac{\Phi_s}{L_s} \end{cases} \tag{15}$$

From vector control conditions, the stator voltage can be expressed as:

$$V_s = \omega_s . \Phi_s \tag{16}$$

Then, the final vector control equations of the rotor's voltage are:

$$\begin{cases} v_{dr} = r_r i_{dr} + \left(L_r - \dfrac{L_m^{\,2}}{L_s} \right) \dfrac{di_{dr}}{dt} - s\omega_s \left(L_r - \dfrac{L_m^{\,2}}{L_s} \right) i_{qr} \\ v_{qr} = r_r i_{qr} + \left(L_r - \dfrac{L_m^{\,2}}{L_s} \right) \dfrac{di_{qr}}{dt} + s\omega_s \left(L_r - \dfrac{L_m^{\,2}}{L_s} \right) i_{dr} + s\omega_s \dfrac{L_m V_s}{\omega_s L_s} \end{cases} \tag{17}$$

2. DFIG's Control

The Rotor Side Converter (RSC) is used to control both active and reactive powers provided by the stator of the DFIG. The control strategy of the RSC is based on the power vector control of the DFIG, and the principle of this control is illustrated by Fig. 5. Different controllers can be used for this purpose.

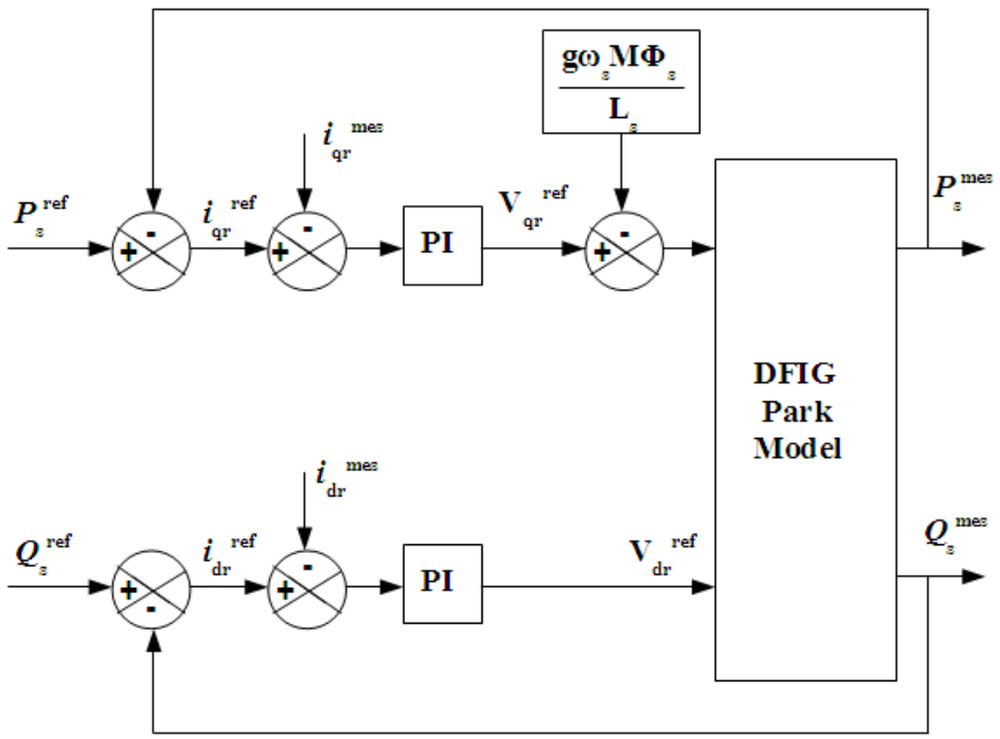

Figure 5. Scheme of the power control vector of the DFIG

The Grid Side Converter (GSC) is used to regulate the DC-link voltage and to adjust the power factor. The GSC is a bidirectional converter which operates as a rectifier when the slip (g) is positive (subsynchronous mode) and as an inverter when the slip is negative (oversynchronous mode).

The active and reactive powers on the grid side are written respectively as follows (X. Yao et al. 2008):

$$\begin{cases} P = \frac{3}{2} V_m . i_d \\ Q = -\frac{3}{2} V_m . i_q \end{cases} \tag{18}$$

$V_m$isthe magnitude of voltage of the grid. The principle of control of GSC is illustrated by Fig. 6.

http://dx.doi.org/10.5772/52341

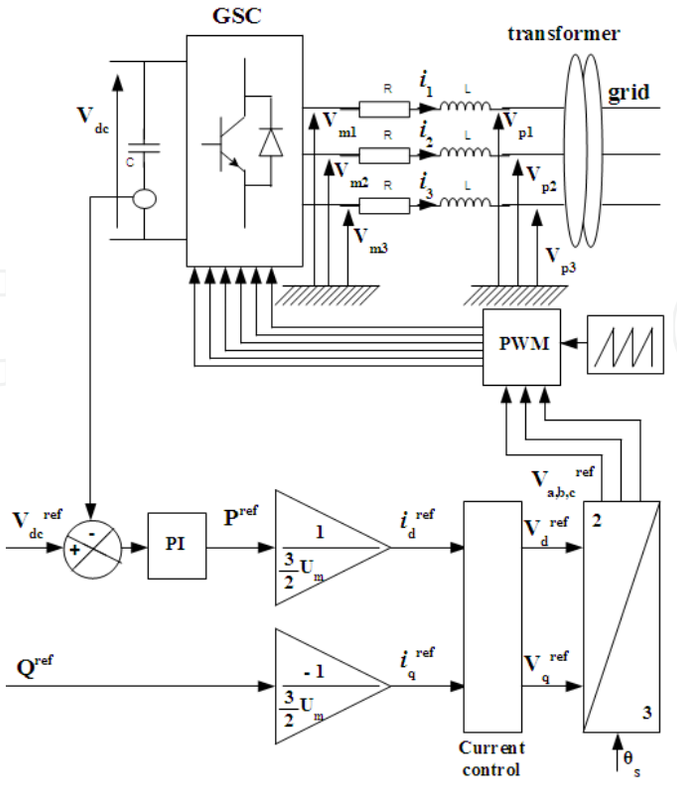

Figure 6. Scheme of the GSC converter control

2.3. Diesel generator modelling

The diesel ge4narator is composed of the diesel engine and Wound Rotor Synchronous Generator (WRSG).

a. Diesel Engine

The model of the diesel engine is shown in Fig. 7 (R. Dettmer, 1990; R. Pena et al., 2002; S. Roy et al., 1993). The dynamic of the actuator is modeled by a first order model with time constant $\tau_1$and gain K_1 (R. Pena et al., 2008; S. Roy et al., 1993). The combustion bloc is represented with gain K_2 and delay τ_2(R. Dettmer, 1990).

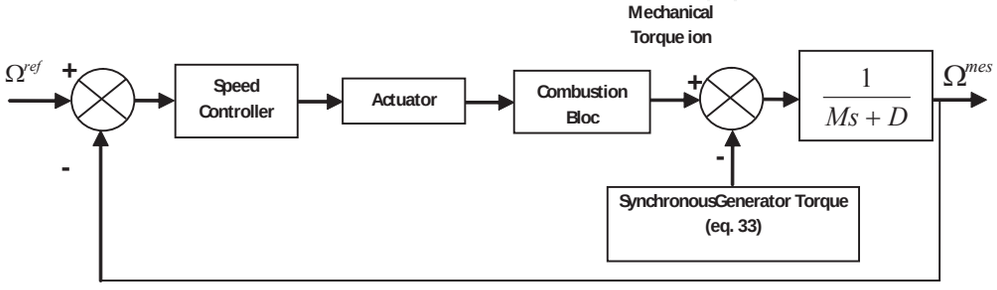

Figure 7. Block diagram of diesel generator model

The actuator is modelled as:

$$\frac{K_1}{1+s\tau_1} \tag{19}$$

The model of the combustion bloc is given by:

$$K_2 e^{-s\tau_2} \tag{20}$$

The delay can be expressed as (R. Pena et al., 2002; R. Pena et al., 2008):j

$$\tau_2 = \frac{60h}{2Nn_c} + \frac{60}{4N} \tag{21}$$

h represents the strokes number, n_c the number of cylinders and N the speed of diesel generator (rpm), Φ is the fuel consumption rate (kg/sec) (F. Jurado and J. R. Saenz, 2002). In the order to maintain constant the frequency of the grid (AC-bus), the speed of the diesel engine must be kept constant when the load varies.

2. Synchronous Generator

The simplified model of the Wound RotorSynchronous Generator (WRSG) can be obtained in *dq* frame (conversion between *abc* and *dq* can be realized by means of the Park Transform) (T. Burton et al., 2001).

The stator armature windings voltages are:

$$\begin{cases} v_d = -R_s i_d + \dfrac{d\lambda_d}{dt} - \omega\lambda_q \\ v_q = -R_s i_q + \dfrac{d\lambda_q}{dt} + \omega\lambda_d \end{cases} \tag{22}$$

R_s is the stator winding resistance

The stator fluxes are

$$\begin{cases} \lambda_d = -L_d i_d + L_{md}\left(i_f + i_D\right) \\ \lambda_q = -L_q i_q + L_{mq} i_Q \end{cases} \tag{23}$$

http://dx.doi.org/10.5772/52341

Rotor armature winding voltage is

$$v_f = -R_f i_f - L_d \frac{di_d}{dt} + L_f \frac{di_f}{dt} + L_{md} \frac{di_D}{dt} \tag{24}$$

Damper windings are characterized by

$$\begin{cases} 0 = R_D i_D - L_{md} \dfrac{di_d}{dt} + L_{md} \dfrac{di_f}{dt} + L_D \dfrac{di_D}{dt} \\ 0 = R_Q i_Q - L_{mq} \dfrac{di_q}{dt} + L_Q \dfrac{di_Q}{dt} \end{cases} \tag{25}$$

To eliminate v_d and v_q in the expression of the stator voltages, we introduced the R_cL_c load which is supplied by the synchronous generator.

$$\begin{cases} v_d = R_c i_d + L_c \dfrac{di_d}{dt} - \omega L_c i_q \\ v_q = R_c i_q + L_c \dfrac{di_q}{dt} + \omega L_c i_d \end{cases} \tag{26}$$

By using the equations above, the state space model of the Wound Rotor Synchronous Generator (WRSG) can be written as follow (Belmokhtar et al., 2012a, Belmokhtar et al., 2012b)):

$$[\dot{X}] = [A].[X] + [B].[U] \tag{27}$$

Where

$[A]$: State matrix; $[X]$: State vector; $[B]$: Control matrix; $[U]$: Control vector.

$[X]=[i_d i_q\ i_f i_D i_Q]^T$ and $[B]=[0\ 0\ 0\ v_f\ 0\ 0]^T$

$$\begin{aligned} \frac{di_d}{dt} &= \left(\frac{1}{L_c + \left(\alpha - \dfrac{\alpha\beta}{\chi} \right)} \right) \left(\begin{array}{l} -(R_s + R_c) i_d + \omega (L_q + L_c) i_q + \dfrac{\beta}{\chi} V_f + \\ \dfrac{\beta}{\chi} R_f i_f + \left(\dfrac{\beta}{\chi} - 1 \right) \dfrac{L_{md}}{L_D} R_D i_D - \omega L_{mq} i_Q \end{array} \right) \\ \frac{di_q}{dt} &= \left(\frac{1}{L_c + \gamma} \right) \left(\begin{array}{l} -\omega (L_d + L_c) i_d - (R_s + R_c) i_q + \omega L_{md} i_f + \\ \omega L_{md} i_D - \dfrac{L_{mq}}{L_Q} R_Q i_Q \end{array} \right) \end{aligned} \tag{28}$$

$$\frac{di_f}{dt} = -\frac{\alpha(R_s + R_c)}{\chi\delta} i_d + \frac{\omega\alpha(L_q + L_c)}{\chi\delta} i_q + \left(\left(\frac{\alpha\beta}{\chi^2\delta} R_f\right) + \left(\frac{R_f}{\chi}\right)\right) i_f + \left(\frac{1}{\chi} + \frac{\alpha\beta}{\chi^2\delta}\right) V_f + \left(\left(\frac{\beta}{\chi} - 1\right)\frac{\alpha}{\delta\chi} + \frac{1}{\chi}\right)\frac{L_{md}}{L_D} R_D I_D - \frac{\omega\alpha L_{mq}}{\chi\delta} i_Q$$

$$\frac{di_D}{dt} = \frac{L_{md}(R_s + R_c)}{L_D\delta}\left(\left(\frac{\alpha}{\chi}\right) - 1\right) i_d + \frac{\omega L_{md}(L_q + L_c)}{L_D\delta}\left(1 - \left(\frac{\alpha}{\chi}\right)\right) i_q - \frac{L_{md}R_f}{L_D\chi}\left(1 + \left(\frac{\alpha\beta}{\chi\delta}\right) + \frac{\beta}{\delta}\right) i_f - \frac{L_{md}}{L_D}\left(\frac{1}{\chi} + \left(\frac{\alpha\beta}{\chi^2\delta}\right) + \frac{\beta}{\chi\delta}\right) V_f - \left(\left(\left(\frac{\beta}{\chi} - 1\right)\left(\frac{\alpha}{\delta\chi} - \frac{1}{\delta}\right) + \frac{1}{\chi}\right)\frac{L_{md}^2}{L_D^2} + \frac{1}{L_D}\right) R_D i_D + \left(\frac{L_{md}}{L_D}\frac{\omega\alpha L_{mq}}{\chi\delta} - \left(\frac{\omega L_{md}L_{mq}}{\delta L_D}\right)\right) i_Q \tag{29}$$

$$\frac{di_Q}{dt} = -\omega\frac{L_{mq}(L_d + L_c)}{L_Q(L_c + \gamma)} i_d - \frac{L_{mq}(R_s + R_c)}{L_Q(L_c + \gamma)} i_q + \omega\frac{L_{mq}L_{md}}{L_Q(L_c + \gamma)} i_f + \omega\frac{L_{md}L_{mq}}{L_Q(L_c + \gamma)} i_D - \left(\frac{L_{mq}^2}{L_Q^2(L_c + \gamma)} + \frac{1}{L_Q}\right) R_Q i_Q$$

$$T_{em} = p\left(\left(L_d - L_q\right) i_d i_q + L_{md} i_f i_q + L_{md} i_q i_D - L_{mq} i_d i_Q\right)$$

P is the number of the poles

In order to improve the efficiency and avoid wet stacking, a minimum load of about 30% to 40% is usually recommended by the manufacturers (J. B. Andriulli et al., 1999). To achieve this goal, the values of R_c and L_c are chosen in the aim to give 35% of the rated power of the diesel generator when it is switched on. Then the partial values of the stator currents i_{d0} and i_{q0} in the dq frame are calculated. The additional values of the stator currents i_{d1} and i_{q1} are computed respectively as follow:

$$\begin{cases} i_{d1} = \dfrac{v_d P_{diesel}^{Add} - v_q Q_{diesel}^{Add}}{\dfrac{3}{2}\left(v_d^2 + v_q^2\right)} \\ i_{q1} = \dfrac{v_q P_{diesel}^{Add} + v_d Q_{diesel}^{Add}}{\dfrac{3}{2}\left(v_d^2 + v_q^2\right)} \end{cases} \tag{30}$$

The active additional power and the reactive power of the diesel generator are expressed respectively as:

http://dx.doi.org/10.5772/52341

$$\begin{cases} P_{diesel}^{Add} = \frac{3}{2}\left(v_d.i_{d1} + v_q.i_{q1}\right) \\ Q_{diesel}^{Add} = \frac{3}{2}\left(v_d.i_{q1} - v_q.i_{d1}\right) \end{cases} \quad (31)$$

The total stator currents of the diesel generator are:

$$\begin{cases} i_{dt} = i_{d0} + i_{d1} \\ i_{qt} = i_{q0} + i_{q1} \end{cases} \quad (32)$$

Then, (27) is expressed as follow:

$$T_{em} = p\left(\left(L_d - L_q\right)i_{dt}i_{qt} + L_{md}i_f i_{qt} + L_{md}i_{qt}i_D - L_{mq}i_{dt}i_Q\right) \quad (33)$$

The diesel generator will operate with minimum load of 35% of the rated power. The alkaline electrolyzers are used as dump load. The electrolyzers are supplied by the surplus power, and then contribute to balance the load demand and power production.

2.4. Alkaline electrolyzer

The decomposition of water into hydrogen and oxygen can be obtained by passing a direct electric current (DC) between two electrodes separated by a membrane and containing an aqueous electrolyte with good ionic conductivity. The electrodes are immersed in an alkaline aqueous solution.

The electrolyzer model is composed of several modules (F. J. Pino et al., 2011). Powered by the DC electrical sources and pure water, an electrolyzer can effectively split water into hydrogen and oxygen. Since it is difficult to obtain analytically the inverse of the equation (34), linear models are used generally in literature (R.Takahashi et al. 2010).

In this paper, the electrolyzer model takes into account the ohmic resistances and cell overvoltages (equation 34) (O. Ulleberg, 1998).

$$V_{cell} = E_0 + \frac{r_1 + r_2 T_{ele}}{A_{ele}} I_{ele} + s_0 \log\left(\frac{t_1 + t_2 / T_{ele} + t_3 / T_{ele}^2}{A_{ele}} + 1\right) \quad (34)$$

$$s_0 = s_1 + s_2 T_{ele} + s_3 T_{ele}^2 \quad (35)$$

$V_{rev}$is the reversible voltage, r_i, $s_i$and t_i are the empirical parameters whose values are determined from experiments (N. Gyawali and Y. Oshsawa, 2010).

The electrolyzer's voltage is expressed as:

$$V_{ele} = N_c.V_{cell} \tag{36}$$

$V_{cell}$is the voltage of electrolyzer cell and N_c is the number of cells of the electrolyzer.

3. Hybrid power system simulation results

The load's power, diesel genset's power and wind generators power are shown respectively in Fig. 8, Fig. 9 and Fig. 10. The diesel genset operates with minimum load of 35% of the rated power (Fig. 9). Three 80 kW alkaline electrolyzers are used as dump load. The surplus power is absorbed bythe electrolyzers (Fig. 11, Fig. 12, Fig. 13) which contribute to balance the load demand and power production (Fig. 14). Electrolyzers contribute to maintain the frequency of the autonomous power system (Fig. 15).

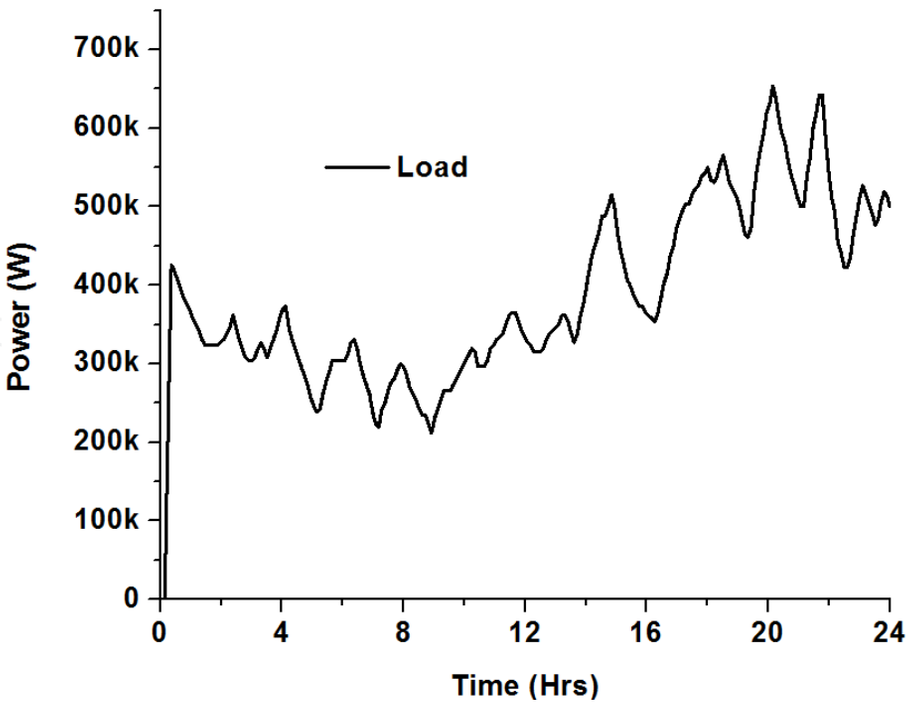

Figure 8. Load profile

http://dx.doi.org/10.5772/52341

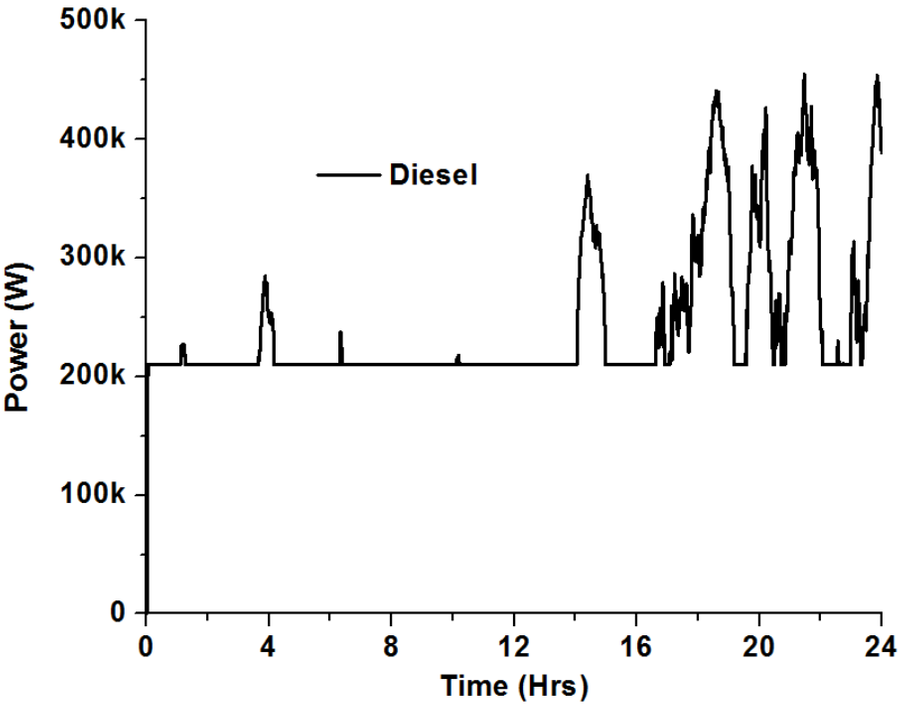

Figure 9. Diesel genset power

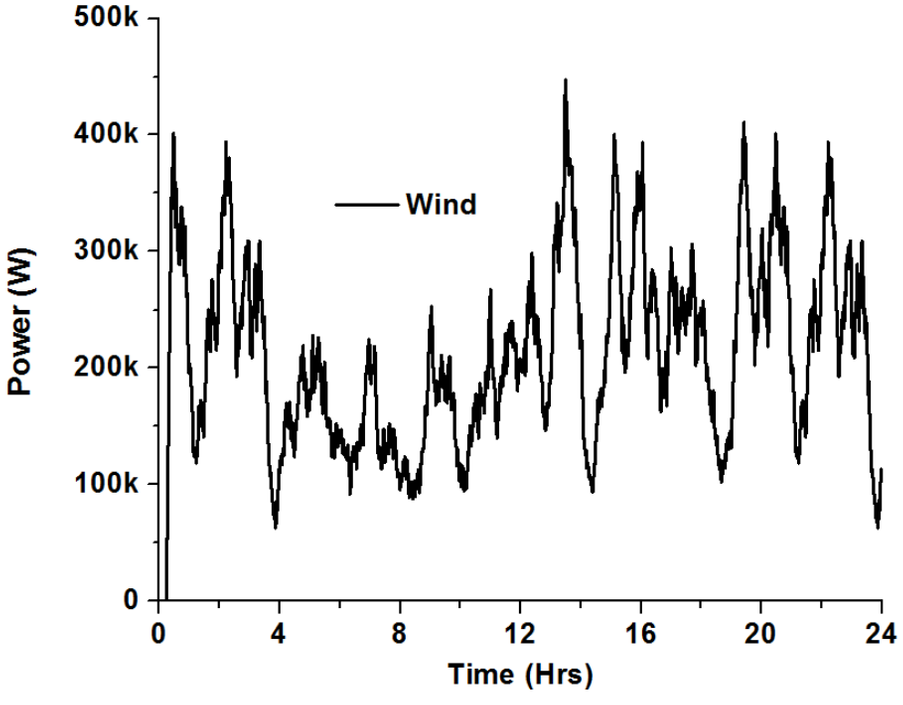

Figure 10. Wind farm power

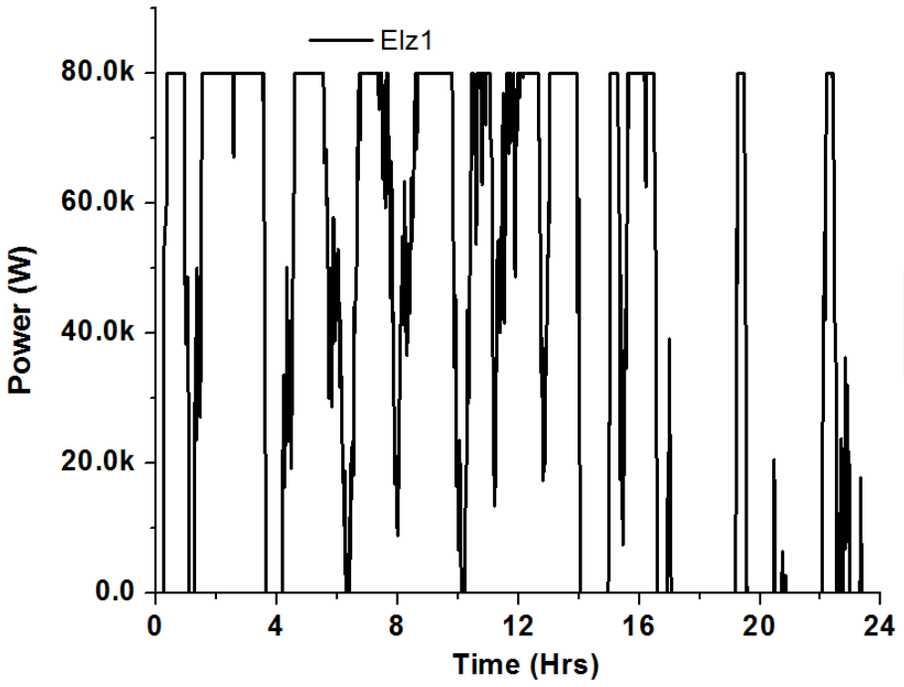

Figure 11. Power absorbed by Electrolyzer 1

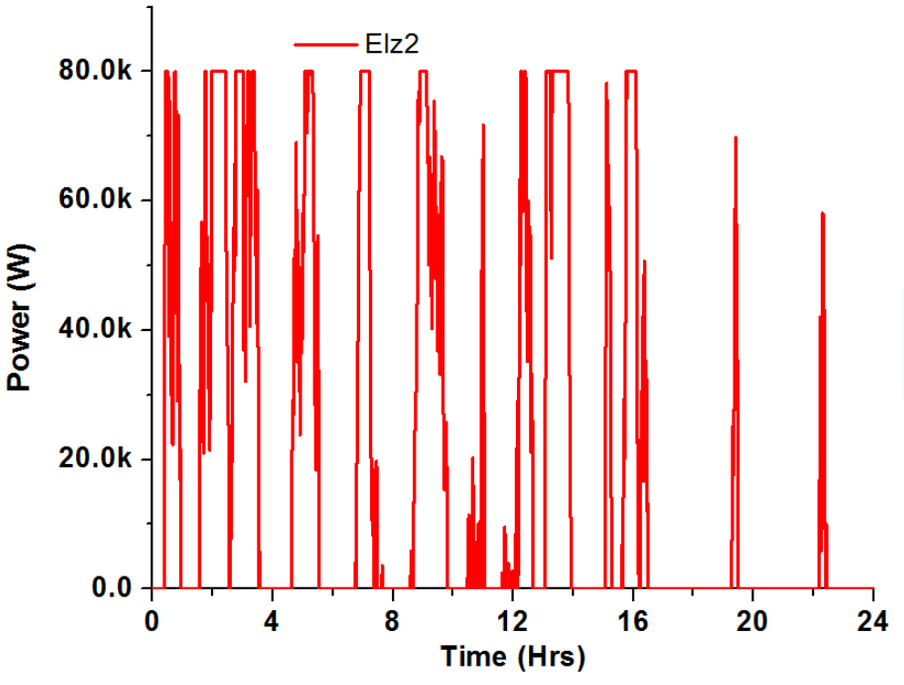

Figure 12. Power absorbed by Electrolyzer 2

http://dx.doi.org/10.5772/52341

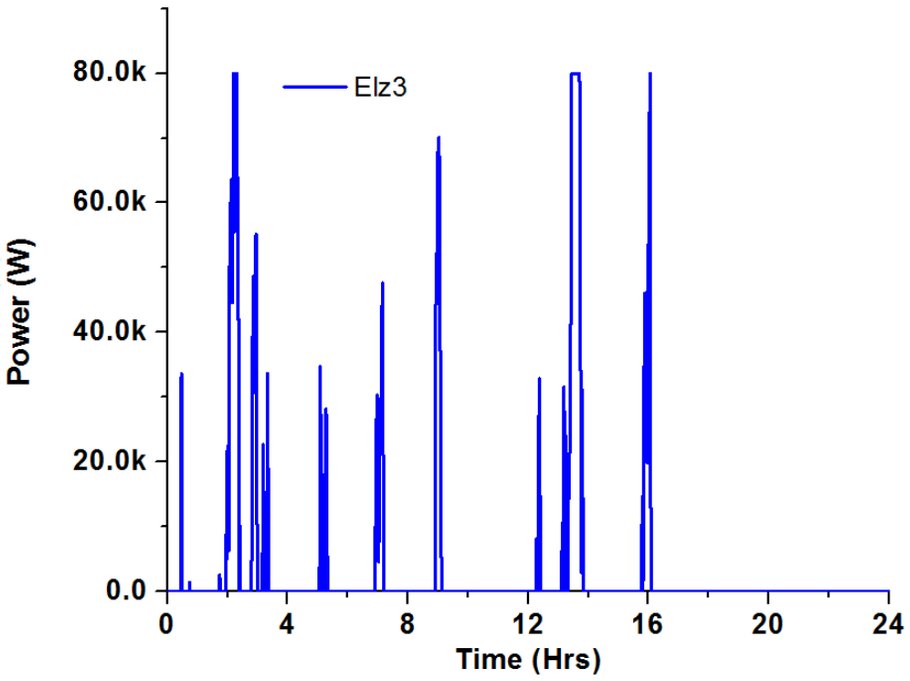

Figure 13. Power absorbed by Electrolyzer 3

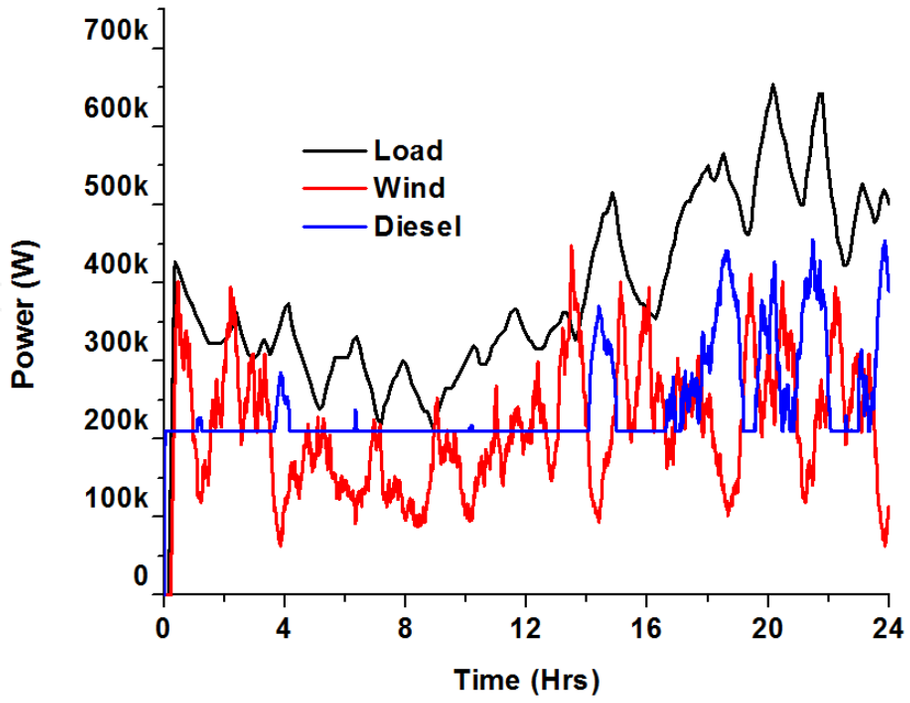

Figure 14. wind, diesel and Load powers

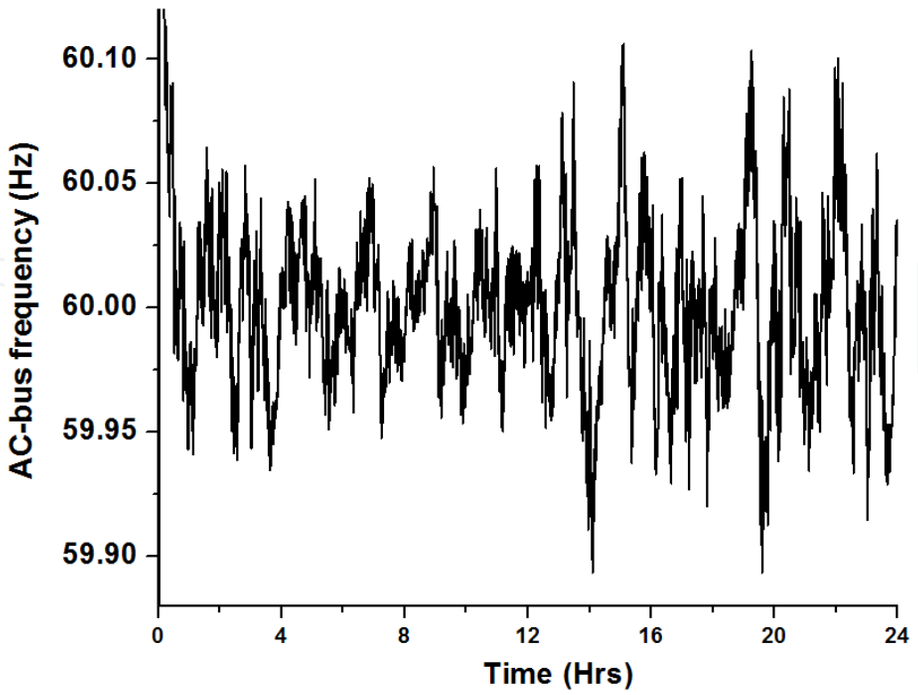

Figure 15. AC-bus frequency

4. Conclusion

This chapter is devoted to a large scale wind diesel Hybrid Power System (HPS). It presents theoretical analysis, modelling and control of Wind Energy Conversion Systems (WECS) connected to an autonomous power system with hydrogen storage. The wind generator under study is a Doubly Fed Induction Generator (DFIG) type. The models of the main components (mainly wind turbine, generator, diesel generator, electrolyzer) are derived. Power transfer strategy in the interconnected system was presented. The effectiveness of the proposed control strategy was validated by simulation using Matlab/ Simulink/ SimPowerSystems environment.

Author details

Mamadou Lamine Doumbia, Karim Belmokhtar and Kodjo Agbossou

Hydrogen Research Institute, Department of Electrical and Computer Engineering, Université du Québec à Trois-Rivières, Québec, Canada

References

[1] International Energy Agency (IEA)(2008). Energy Technology Perspectives 2008, , 5.

[2] Vaughn Nelson,(2009). WIND ENERGY: Renewable Energy and the Environment, CRC Press, 2009.

[3] US Department of Energy(2011). Wind Technologies Market Report 2010, June 2011.

[4] Zoulias, E. I., & Lymberopoulos, N. (2008). Hydrogen-based Autonomous Power Systems, Springer-Verlag.

[5] Nelson et al.(2006). Unit sizing and cost analysis of stand-alone hybrid wind/PV/fuel cell power generation system. Renewable Energy , 31, 1641-1656.

[6] MamadouLamineDoumbia and KodjoAgbossou,"Photovoltaic/Wind energy system with hydrogen based",Renewable Energy, ISBN 978-953-7619-52-7, 2009.

[7] K. Agbossou, M. Kolhe, J. Hamelin and T.K. Bose, « Performance of Stand-alone Renewable Energy System based on Energy Storage as Hydrogen », IEEE Transactions on Energy conversion, vol. 19, no 3, p. 633-640, 2004.

[8] Tao Zhou,(2009). Commande et Supervision Energétique d'un Générateur Hybride Actif Eolien incluant du Stockage sous forme d'Hydrogène et des Super-Condensateurs pour l'Intégration dans le Système Electrique d'un Micro Réseau, thèse de doctorat, 2009, École Centrale de Lille, France.

[9] Munteanu, I., Bratcu, A. I., -A, N., Cutululis, , Ceanga, E., & (2008).", . (2008). Optimal Control of Wind Energy Systems".Springer 2008.

[10] Miller, N. M., Price, W. W., Sanchez-Gasca, J. J., & (2003).", . (2003). Dynamic Modelling of GE 1.5 and 3.6 Wind Turbine-Generators".GE-Powwer Systems Energy Consulting, General Electric International, Inc, Schenectady, NY, USA, Oct, 27, 2003.

[11] Heier, S. (1998). Grid Integration of Wind Energy, Conversions Systems", John Wiley & Sons Ltd, New-York 1998.

[12] Qiao, W., Zhou, W., Aller, J. M., & Harley, R. G. (2008). Wind Speed Estimation Based Sensorless Output Maximization Control for a Wind Turbine Driving a DFIG". IEEE Trans. Power Electron., May 2008., 23(3), 1156-1169.

[13] Thomas Ackermann(2005). Wind Power in Power Systems, John Wiley & Sons, Ltd.

[14] Ren, Y., Li, H., & Zhou, J. (2009). Dynamic Performance of Grid-Connected DFIG Based on Fuzzy Logic Control", Proceeding of the 2009, International Conference on Mechatronics and Automation, August, China, 2009., 9-12.

[15] De Almeida, R. G., Lopes, J. A. P., & Barreiros, J. A. L. (2004). Improving Power System Dynamic Behavior Through Doubly Fed Induction Machines Controlled by Static Converter Using Fuzzy Control", IEEE Trans. on Power Systems. November 2004., 19(4), 1942-1950.

[16] Aouzellag, K., Ghedamsi, , & Berkouk, E. M. (2006). Power Control of a Variable Speed Wind Turbine Driving an DFIG", in ICREPQ06, (220)

[17] Yao, X., Yi, C., Ying, D., Guo, J., & Yang, L. (2008). The grid-side PWM Converter of the Wind Power Generation System Based on Fuzzy Sliding Mode Control", AdvancedIntelligent Mechatronics, IEEE 2008, Xian (Chine), , 973-978.

[18] Dettmer, R. (1990). Revolutionary energy-A wind/diesel generator with flywheel storage".Inst. Electr. Eng. Rev., Apr. 1990., 36, 149-151.

[19] Pena, R., Cardenas, R., Clare, J., & Asher, G. (2002). Control strategy of doubly fed generators for a wind diesel energy system". IECON 02, , 4, 3297-3302.

[20] Roy, S., Malik, O. P., & Hope, G. S. (1993). A k-Step Predictive Scheme for Speed Control of Diesel Driven Power Plants". IEEE Trans. Ind. Appl., , 29(2), 389-396.

[21] Pena, R., Cardenas, R., Proboste, J., Clare, J., & Asher, G. (2008). Wind-Diesel Generation Using Doubly Fed Induction Machines". IEEE Trans. Energy. Convers., March. 2008., 23(1), 202-213.

[22] Jurado, F., & Saenz, J. R. (2002). Neuro-fuzzy control for autonomous wind-diesel systems using biomass".Renewable.Energy 27, , 39-56.

[23] Burton, T., Sharpe, D., Jenkins, N., & Bossanyi, E. (2001). Wind Energy Handbook".John Wiley & Sons, Ltd, 2001.

[24] KarimBelmokhtar et al.(2012a). Modelling and Fuzzy Logic Control of DFIG Based Wind Energy Conversion Systems". IEEE SPEEDAM Conference, Sorrento, Italy, 2012.

[25] KarimBelmokhtar et al.(2012b). New Sensorless Fuzzy Logic Control Strategy of Wind Energy Conversion Systems".IEEE ISIE Conference, Hangzhou, China, 2012.

[26] Andriulli, J. B., Gates, A. E., Haynes, H. D., Klett, L. B., Matthews, S. N., Nawrocki, E. A., Otaduy, P. J., Scudiere, M. B., Theiss, T. J., Thomas, J. F., Tolbert, L. M., Yauss, M. L., & Voltz, C. A. (1999). Advanced power generation systems for the 21st century: Market survey and recommendations for a design philosophy," Oak Ridge National Laboratory, Oak Ridge, TN, Tech. Rep. Nov. 1999.

[27] Pino, F. J., Valverde, L., & Rosa, F. (2011). Influence of wind turbine power curve and electrolyser operating temperature on hydrogen production in wind-hydrogen systems". Journal of Power Sources, , 196(9), 4418-4426.

[28] Takahashi, R., Kinoshita, H., Murata, T., Tamura, J., Sugimasa, M., Komura, A., Futami, M., Ichinose, M., & Ide, K. (2010). Output Power Smoothing and Hydrogen Production by Using Variable Speed Wind Generators".IEEE Transactions on Industrial Electronics, , 57(2), 485-493.

[29] Ulleberg, O. (1998). Stand-alone power systems for the future: optimal design, operation & control of solar-hydrogen energy systems", PhD Thesis, (1998).

[30] Gyawali, N., & Ohsawa, Y. (2010). Integrating Fuell Cell/ Electrolyzer/ Ultracapacitor System Into a Stand-Alone Microhydro Plant". IEEE Transactions on Energy Conversion, ., 25(4), 10921-11101.

IntechOpen

IntechOpen